Inorganic Chemistry
Cite This: Inorg. Chem. 2019, 58, 2270−2274
Communication
pubs.acs.org/IC

From Pincer to Paddlewheel: C−H and C−S Bond Activation at Bis(2-pyridylthio)methane by Palladium(II)

Partha Halder, Daniel J. SantaLucia, Sungho V. Park, and John F. Berry*

Department of Chemistry, University of Wisconsin—Madison, 1101 University Avenue, Madison, Wisconsin 53706, United States

Supporting Information

ABSTRACT: The bis(2-pyridylthio)-methanidopalladium(II) pincer complex (**1**), containing a Pd−C bond, was obtained from the reaction of bis(2-pyridylthio)methane (H_2L) with palladium(II) acetate in toluene under reflux. When palladium(II) trifluoroacetate was used, H_2L reacted to generate the tetrakis(pyridine-2-thiol)palladium(II) complex (**2**). Complex **2** was converted to a heterobimetallic palladium(II)−iron(II) paddlewheel complex (**3**) upon treatment with iron(II) triflate in the presence of a base in acetonitrile at room temperature.

Downloaded via UNIV OF WISCONSIN-MADISON on March 12, 2019 at 14:42:42 (UTC).
See https://pubs.acs.org/sharingguidelines for options on how to legitimately share published articles.

Palladium pincer complexes have contributed much to the development of organometallic catalysis.[1] Carbon-donor pincers generally involve N-heterocyclic carbenes or aromatic carbanions,[1d,f−i] and examples of palladium pincer complexes featuring a donating sp^3-hybridized carbon atom are limited.[2]

Toward the study of C(sp^3)−H bond activation by palladium(II), we have synthesized and characterized a mononuclear palladium pincer complex of the bis(2-pyridylthio)methane (H_2L) ligand. This ligand has been shown to form mononuclear or polynuclear coordination complexes with a variety of metal ions.[3] However, to the best of our knowledge, this is the first example of a direct M−C(sp^3)-bonded pincer complex with this ligand. Furthermore, we were surprised to find that activation of the C(sp^3)−S bond of the ligand provides tetrakis(pyridine-2-thiol)palladium(II) (**2**; CCDC 1860814), which acts as a precursor to the heterobimetallic paddlewheel complex $Pd^{II}Fe^{II}(PyS)_4(CH_3CN)$ (**3**; CCDC 1860815), featuring a partial Pd^{II}−Fe^{II} metal−metal bond. Complexes that contain heterometallic metal−metal bonds are increasingly being employed as molecular magnets and sensing materials and for addressing important challenges in biology, energy, and catalysis.[4] We report herein the use of H_2L as a precursor to either a pincer or a paddlewheel complex, depending on the Pd source used.

The reaction between $Pd(OAc)_2$ and H_2L (derived from pyridine-2-thiol, PySH) in toluene under reflux affords a brown complex, $[Pd^{II}(HL)(OAc)]\cdot AcOH$ (**1**·AcOH; CCDC 1860813), in 43% yield via C−H bond activation (Scheme 1a).

The electrospray ionization mass spectrometry (ESI-MS) spectrum of **1** in methanol shows signals at m/z 338.924 and 398.945 with the expected isotope distributions calculated for $[Pd(HL)]^+$ and $[Pd(HL)(OAc)]^+$, respectively (Figure S1). ^1H NMR spectroscopy in $CDCl_3$ shows that the complex is diamagnetic (Figure S2). The aliphatic proton signal shifts from 5.06 to 6.20 ppm with respect to the free ligand, and this shift is large compared to the shifts observed for the pyridine protons. This large shift is due to formation of the Pd−C bond in **1**.

Scheme 1. (a) Syntheses of Mononuclear Palladium(II) and Heterobimetallic Palladium(II)−Iron(II) Complexes and (b) Tautomeric and Resonance Forms of PySH

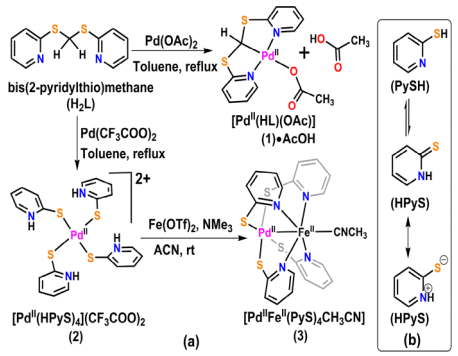

X-ray quality single crystals of **1**·AcOH were grown by slow diffusion of pentane into a toluene solution of the complex at 298 K under an inert atmosphere. The complex crystallizes in the monoclinic space group $C2/c$ (Table S1). The crystal structure reveals a square-planar geometry of the palladium center bonded to the monoanionic NCN-donor ligand (HL^-) and to a monodentate acetate ligand (Figure 1a). The anionic carbon (C6) and one acetate oxygen (O1) coordinate to the palladium center *trans* to each other with a Pd1−C6 distance of 1.986(4) Å. The Pd1−O1 bond [2.112(3) Å] is longer than expected (ca. 2.041 Å)[5] because of the *trans* influence of the

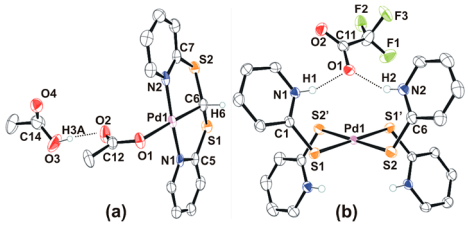

Figure 1. Thermal ellipsoid plots with ellipsoids drawn at the 50% probability level for (a) **1**·AcOH and (b) **2**. All hydrogen atoms are omitted except the acetic acid hydrogen atom and the ones bound to the pyridinium nitrogen atoms. Only one CF_3COO^- anion is shown for **2**.

Received: December 21, 2018
Published: January 30, 2019

© 2019 American Chemical Society

DOI: 10.1021/acs.inorgchem.8b03568
Inorg. Chem. 2019, 58, 2270−2274

carbanionic ligand[2b] (Table S2). The other oxygen atom of the acetate ligand forms a strong hydrogen-bonding interaction with one molecule of acetic acid with a O3···O2 distance of 2.602(6) Å (Table S2). The coordinated acetate ion and noncoordinated acetic acid molecule exchange quickly on the NMR timescale at room temperature. Using variable-temperature ^{13}C NMR spectroscopy, we find that the two separate acetate groups are distinguishable below −15 °C (Figure S3). This result emphasizes the *trans* effect of the Pd−C(sp^3) bond.

Interestingly, the reaction of H_2L with $Pd(CF_3COO)_2$ does not yield an analogue of **1** but instead gives the dark-orange complex $[Pd^{II}(PySH)_4](CF_3COO)_2$ (**2**) in 15% yield (Scheme 1a) and insoluble black residue. Oxidative C−S bond activation of H_2L has been shown to occur with anions of copper(II) salts, but this is the first example with palladium.[3a] Umakoshi et al. have synthesized an analog of **2** with chloride counteranions in 77% yield by the reaction of $[PdCl_2(CH_3CN)_2]$ and PySH at high temperatures in dioxane.[6] Here, an alternate synthesis of **2** was carried out with PySH and palladium(II) trifluoroacetate in acetonitrile at room temperature, which gives **2** in 90% yield. The IR spectrum of **2** shows bands at around 1191−1130 cm^{-1} attributable to ν(C−F) stretches of the trifluoroacetate counteranion. Complex **2** has signals at m/z 274.98 and 662.95 in its ESI-MS spectrum, each consistent with the expected isotope distributions calculated for $[Pd(PySH)_4]^{2+}$ and $[Pd(PySH)_4(CF_3COO)]^{+}$, respectively (Figure S4). The diamagnetic complex **2** was further characterized by ^1H NMR spectroscopy in CD_3CN, which shows peaks between 8.18 and 7.21 ppm for the pyridine protons (Figure S5). The broad peak at 14.85 ppm is assigned to the NH protons.

The X-ray crystal structure of **2** reveals a four-coordinate square-planar geometry at the palladium center with HPyS ligands (Figure 1b). The Pd−S bond lengths vary in the range of 2.3326(7)−2.3269(7) Å, and C−S bond lengths vary strictly from 1.716(2) to 1.713(2) Å (Table S3). These lengths are comparable to those in palladium tetrathiolate complexes.[6,7] The short Pd−S bond distances are indicative of monoanionic thiolates (instead of thiones) bound to the palladium(II) center like other metal−PySH complexes.[8] Thus, the PySH ligands in **2** bind in a zwitterionic form, HPyS (bottom, Scheme 1b). All of the protonated pyridinium nitrogen atoms participate in strong hydrogen-bonding interactions with the trifluoroacetate counterions with N1···O1 and N2···O1 distances of 2.763(2) and 2.797(3) Å, respectively (Table S3).

The reaction of **2** and $Fe(OTf)_2$ in acetonitrile, followed by treatment with trimethylamine (Me_3N) at room temperature under an inert atmosphere yields an orange-red complex, **3** (Scheme 1a). This is an improvement from the conditions used by Kinoshita et al., who synthesized platinum-based heterobimetallic complexes with first-row transition metals and a PySH derivative at higher temperatures in sealed-tube reactions.[9] Wagler and co-workers synthesized rhodium−antimony heterobimetallic paddlewheel complexes with this ligand, but these are insoluble in common organic solvents.[10] The matrix-assisted laser desorption/ionization MS (MALDI-MS) of **3** shows a signal at m/z 603.521 with the expected isotope distribution for $[PdFe(PySH)_4]^+$ (Figure S6). The ^1H NMR spectrum of complex **3** in CD_3CN at room temperature shows sharp peaks for the pyridine protons with paramagnetic shifts (Figure S7) consistent with retention of the paddlewheel structure in solution and the presence of high-spin iron(II).[11]

The structure of **3** reveals four sulfur atoms coordinated to the palladium center, with distances similar to those reported for **2**. Four pyridine nitrogen atoms coordinate to the iron center upon deprotonation by Me_3N, forming the (4,0) isomer of the heterobimetallic palladium−iron complex **3** (Figure 2). The

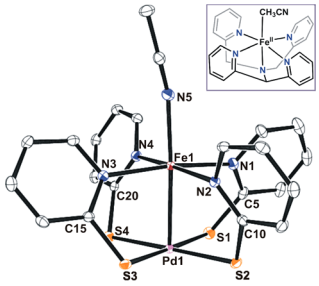

Figure 2. Thermal ellipsoid plots with ellipsoids drawn at the 50% probability level for **3**. All hydrogen atoms are omitted. The inset is the binding motif for the Fe^{II}-N4Py complex.

acetonitrile molecule and palladium center coordinate to the iron atom *trans* to each other, occupying the axial positions with a Pd1−Fe1−N5 angle of 176.66(6)°, a short Fe1−Pd1 distance of 2.595(10) Å, and a Fe1−N5 distance of 2.180(2) Å (Table S4). The Pd−Fe bond distance is comparable to the Pd−Fe bond distances reported recently in Fe−Pd−Fe trimetallic molecules[11b,12] and shorter than that of palladium ferrocenyl complexes, which have Pd−Fe distances ranging from 2.63 to >2.9 Å.[13] The geometry about the iron center is reminiscent of the iron complex with the N4Py ligand (Figure 2, inset), although $[(N4Py)Fe(NCCH_3)]^{2+}$ and its derivatives are all low-spin.[14]

The optical spectrum of the complex **1**·AcOH in acetonitrile under an inert atmosphere exhibits a shoulder at 390 nm (ε = 4300 M^{-1} cm^{-1}) corresponding to a ligand-centered transition. Complex **2** shows an absorption peak at 483 nm (ε = 3600 M^{-1} cm^{-1}), which may be assigned to a metal-to-ligand (palladium(II)-to-thiolate π^*) charge-transfer transition (MLCT; Figure 3). Similarly, complex **3** exhibits an absorption peak at 430 nm

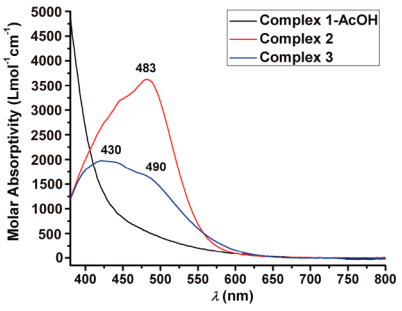

Figure 3. Optical spectra of complexes **1**·AcOH, **2**, and **3** (0.5 mM) in acetonitrile at room temperature under an inert atmosphere.

(ε = 2000 M^{-1} cm^{-1}) and a shoulder at 490 nm (ε = 1700 M^{-1} cm^{-1}) corresponding to an iron(II)-to-pyridine π^* or a palladium(II)-to-thiolate π^* MLCT (Figure 3).

The cyclic voltammogram (CV) of **1**·AcOH shows irreversible oxidation peaks at E = 0.89 and 1.17 V versus ferrocene/ferrocenium (Fc/Fc^+), which are assigned to $[HLPd(OAc)]^{2+/3+}$ and $[HLPd(OAc)]^{3+/4+}$, respectively (Figure S8). The CV of **2** shows irreversible oxidations at 0.42 and 1.22 V, which may be assigned to oxidation at the palladium center for $Pd^{II} \rightarrow Pd^{III}$ and $Pd^{III} \rightarrow Pd^{IV}$, respectively (Figure S9). Similarly, the CV of **3** has an irreversible oxidation at 0.08 V

DOI: 10.1021/acs.inorgchem.8b03568
Inorg. Chem. 2019, 58, 2270−2274

versus Fc/Fc^+ attributed to $[PdFe(PyS)_4]^{4+/5+}$, which may be assigned to an oxidation localized at the iron center. The nature of the CV is similar to that of the previously reported $[(N4Py)Fe(NCCH_3)]^{2+}$.[15] Moreover, the additional oxidations at 0.47 and 1.62 V attributed to $[PdFe(PyS)_4]^{6+/5+}$ and $[PdFe(PyS)_4]^{7+/6+}$ may both be assigned to oxidations localized at the palladium center (Figure S10).

Magnetic susceptibility data (plotted as χT vs T) for **3** are modeled as an $S = 2$ system. A sharp downward feature is seen in the χT versus T plot below 50 K, indicative of zero-field splitting (Figure S11). The data were fitted with $g_x = g_y = 1.83$, and $g_z = 3.27$; $D = -21.6 \pm 0.26$ cm^{-1} (Table S5).

In addition to the magnetic susceptibility measurement, the solid-state Mössbauer spectrum of **3** was collected at 77 K. The isomer shift and quadruple splitting were 1.087 and 0.995 mm s^{-1}, respectively, indicative of a high-spin iron(II) center within the complex (Figure S12).

Density functional theory calculations further help to evaluate the electronic structure and nature of Pd−Fe bonding in **3**. The S = 2 state is predicted to be more stable compared to the $S = 0$ state by 7.32 kcal mol^{-1}, in agreement with experiments. The molecular orbital (MO) diagram of the $S = 2$ state (Figure 4)

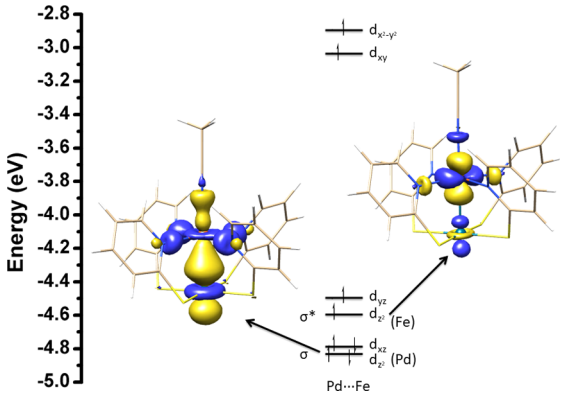

Figure 4. Calculated ground-state MO diagram for **3**. The molecular z axis is along the Pd−Fe bond, and the x and y axes are along Pd−S and Fe−N_{py}, respectively.

indicates a σ-type bonding between palladium and iron involving three electrons, a two-center three-electron bond.[16] The σ-bonding orbital is polarized toward palladium, while the σ^* has more iron character. The four unpaired 3d electrons of iron exist mostly localized at d_{xy}, d_{yz}, $d_{x^2-y^2}$, and d_{z^2}, with the latter involved in the σ bond to palladium.

In summary, three types of palladium(II) complexes derived from the PySH ligand have been isolated and characterized. The pincer complex **1** contains a rare Pd−C(sp^3) bond within the NCN-donor environment. C−S bond cleavage of the NCN-donor ligand by trifluoroacetic acid forms the zwitterionic monodentate PySH ligand, which yields the square-planar palladium complex **2**. Complex **2** was rationally employed as a precursor in the synthesis of the heterobimetallic palladium−iron complex **3**, taking advantage of hard-soft acid-base theory to target the (4,0) isomer of the complex. Complex **3** has structural similarities with the well-known $[(N4Py)Fe(NCCH_3)]^{2+}$ but is high-spin with $S = 2$. The syntheses reported in this work provide useful insights in designing bioinspired complexes containing metal−metal bonds. Reactivity studies in this direction are presently being carried out in our laboratory.

■ ASSOCIATED CONTENT

Supporting Information

The Supporting Information is available free of charge on the ACS Publications website at DOI: 10.1021/acs.inorgchem.8b03568.

Experimental and technical details, crystal structure description, computational details, tables and additional figures (PDF)

Accession Codes

CCDC 1860813−1860815 contain the supplementary crystallographic data for this paper. These data can be obtained free of charge via www.ccdc.cam.ac.uk/data_request/cif, or by emailing data_request@ccdc.cam.ac.uk, or by contacting The Cambridge Crystallographic Data Centre, 12 Union Road, Cambridge CB2 1EZ, UK; fax: +44 1223 336033.

■ AUTHOR INFORMATION

Corresponding Author

*E-mail berry@chem.wisc.edu (J.F.B.).

ORCID

Partha Halder: 0000-0002-6821-9346
Sungho V. Park: 0000-0002-5949-0548
John F. Berry: 0000-0002-6805-0640

Notes

The authors declare no competing financial interest.

■ ACKNOWLEDGMENTS

We thank the U.S. National Science Foundation (NSF) for support through Grant CHE-1664999. The NMR spectroscopy and computer facilities were supported by the NSF (Grants CHE-1048642 and CHE-0840494, respectively). The MS facilities were supported by the National Institutes of Health (Grant 1S10OD0200221). We thank Michael Roy for making SQUID measurements, Michael Aristov for single-crystal data collection, Heike Hofstetter and Charlie Fry for NMR assistance, and Martha M. Vestling for MALDI-MS assistance. P.H. thanks the SERB and IUSSTF, India, for an Indo−U.S. Postdoctoral Fellowship.

■ REFERENCES

(1) (a) van Koten, G.; Gossage, R. A., Eds.; *The Privileged Pincer-Metal Platform: Coordination Chemistry & Applications*; Springer International Publishing, 2016; p 374. (b) Szabo, K. J.; Wendt, O. F., Eds.; *Pincer and Pincer-Type Complexes: Applications in Organic Synthesis and Catalysis*; Wiley-VCH Verlag GmbH & Co. KGaA, 2014; p 302. (c) Johnson, C.; Albrecht, M. Piano-stool N-heterocyclic carbene iron complexes: Synthesis, reactivity and catalytic applications. *Coord. Chem. Rev.* **2017**, *352*, 1−14. (d) Vivancos, A.; Segarra, C.; Albrecht, M. Mesoionic and Related Less Heteroatom-Stabilized N-Heterocyclic Carbene Complexes: Synthesis, Catalysis, and Other Applications. *Chem. Rev.* **2018**, *118*, 9493−9586. (e) Zell, T.; Milstein, D. Hydrogenation and Dehydrogenation Iron Pincer Catalysts Capable of Metal-Ligand Cooperation by Aromatization/Dearomatization. *Acc. Chem. Res.* **2015**, *48*, 1979−1994. (f) Slagt, M. Q.; van Zwieten, D. A. P.; Moerkerk, A. J. C. M.; Gebbink, R. J. M. K.; van Koten, G. NCN-pincer palladium complexes with multiple anchoring points for functional groups. *Coord. Chem. Rev.* **2004**, *248*, 2275−2282. (g) Marset, X.; De Gea, S.; Guillena, G.; Ramon, D. J. NCN-Pincer-Pd Complex as Catalyst for the Hiyama Reaction in Biomass-Derived Solvents. *ACS Sustainable Chem. Eng.* **2018**, *6*, 5743−5748. (h) Rani, V.; Singh, H. B.; Butcher, R. J. Protic and substituted NCN palladium(II) pincer complexes with 1,3-bis(benzimidazol-2'-yl)-2-bromobenzenes: Structure and catalysis. *J. Organomet. Chem.* **2018**, *859*, 33−43. (i) Rani, V.; Singh, H. B.;

DOI: 10.1021/acs.inorgchem.8b03568
Inorg. Chem. 2019, 58, 2270−2274

Butcher, R. J. Cationic NCN Palladium(II) Pincer Complexes of 5-tert-Butyl-1,3-bis(N-substituted benzimidazol-2'-yl)benzenes: Synthesis, Structure, and Pd···Pd Metallophilic Interaction. *Organometallics* **2017**, *36*, 4741−4752. (j) Khusnutdinova, J. R.; Milstein, D. Metal-Ligand Cooperation. *Angew. Chem., Int. Ed.* **2015**, *54*, 12236−12273.

(2) (a) Schoeler, S.; Merz, K.; Puls, A.; Winter, M.; Dyker, G. Synthesis and Characterization of ortho-Thio-Functionalized Triarylmethyl Palladium Complexes. *Eur. J. Inorg. Chem.* **2015**, *2015*, 53−57. (b) Hoffbauer, M. R.; Comanescu, C. C.; Dymm, B. J.; Iluc, V. M. Influence of the Leaving Group on C-H Activation Pathways in Palladium Pincer Complexes. *Organometallics* **2018**, *37*, 2086−2094. (c) Cui, P.; Comanescu, C. C.; Iluc, V. M. Frustrated Lewis pair-like reactions of nucleophilic palladium carbenes with $B(C_6F_5)_3$. *Chem. Commun.* **2015**, *51*, 6206−6209. (d) Comanescu, C. C.; Iluc, V. M. C-H Activation Reactions of a Nucleophilic Palladium Carbene. *Organometallics* **2015**, *34*, 4684−4692. (e) Comanescu, C. C.; Iluc, V. M. Synthesis and Reactivity of a Nucleophilic Palladium(II) Carbene. *Organometallics* **2014**, *33*, 6059−6064. (f) Shimokawa, R.; Kawada, Y.; Hayashi, M.; Kataoka, Y.; Ura, Y. Oxygenation of a benzyl ligand in SNS-palladium complexes with O2: acceleration by anions or Bronsted acids. *Dalton Trans* **2016**, *45*, 16112−16116. (g) Errington, R. J.; McDonald, W. S.; Shaw, B. L. Transition metal-carbon bonds. Part 54. Complexes of palladium, platinum, rhodium, and iridium with $(Me_3C)_2PCH_2CHMe(CH_2)_3P(CMe_3)_2$. Crystal structures of [2-methyl-1,5-bis(di-tert-butylphosphino)pent-3-yl-C_3 PP']-chloropalladium(II) and -chlorohydridoiridium(III). *J. Chem. Soc., Dalton Trans.* **1982**, 1829−1835.

(3) (a) Belen Lago, A.; Amoedo, A.; Carballo, R.; Garcia-Martinez, E.; Vazquez-Lopez, E. M. Metal coordination and in situ S-C bond cleavage of the bis(2-pyridylthio)methane ligand. *Dalton Trans* **2010**, *39*, 10076−10087. (b) Samanamu, C. R.; Lococo, P. M.; Woodul, W. D.; Richards, A. F. Copper halide clusters and polymers supported by bipodal heteroelemental ligands. *Polyhedron* **2008**, *27*, 1463−1470. (c) Pellei, M.; Lobbia, G. G.; Mancini, M.; Spagna, R.; Santini, C. Synthesis and characterization of new organotin(IV) complexes with polyfunctional ligands. *J. Organomet. Chem.* **2006**, *691*, 1615−1621. (d) Xie, Y.-B.; Bu, X.-H. New Silver(I) Complexes of Pyridyl Dithioether Ligands with Ag-Ag Interactions: Effects of Anions and Ligand Spacers on the Framework Formations of Complexes. *J. Cluster Sci.* **2003**, *14*, 471−482. (e) Bu, X.-H.; Xie, Y.-B.; Li, J.-R.; Zhang, R.-H. Adjusting the Frameworks of Silver(I) Complexes with New Pyridyl Thioethers by Varying the Chain Lengths of Ligand Spacers, Solvents, and Counteranions. *Inorg. Chem.* **2003**, *42*, 7422−7430. (f) Amoedo-Portela, A.; Carballo, R.; Casas, J. S.; Garcia-Martinez, E.; Sanchez-Gonzalez, A.; Sordo, J.; Vazquez-Lopez, E. M. Bis(2-pyridylthio)-methane complexes of cadmium(II) halides. *Polyhedron* **2003**, *22*, 1077−1083. (g) Amoedo-Portela, A.; Carballo, R.; Casas, J. S.; Garcia-Martinez, E.; Sanchez-Gonzalez, A.; Sordo, J.; Vazquez-Lopez, E. M. The crystal structure of bis(2-pyridylthio)methanediiodozinc(II), $[ZnI_2(bpytm)]$. *Main Group Met. Chem.* **2002**, *25*, 311−312. (h) Amoedo-Portela, A.; Carballo, R.; Casas, J. S.; Garcia-Martinez, E.; Gomez-Alonso, C.; Sanchez-Gonzalez, A.; Sordo, J.; Vazquez-Lopez, E. M. The coordination chemistry of the versatile ligand bis(2-pyridylthio)methane. *Z. Anorg. Allg. Chem.* **2002**, *628*, 939−950. (i) Kinoshita, I.; Wright, L. J.; Kubo, S.; Kimura, K.; Sakata, A.; Yano, T.; Miyamoto, R.; Nishioka, T.; Isobe, K. Design and synthesis of copper complexes of novel ligands based on the pyridine thiolate group. *Dalton Trans* **2003**, 1993−2003.

(4) (a) Ren, Z.; Sunderland, T. L.; Tortoreto, C.; Yang, T.; Berry, J. F.; Musaev, D. G.; Davies, H. M. L. Comparison of Reactivity and Enantioselectivity between Chiral Bimetallic Catalysts: Bismuth-Rhodium- and Dirhodium-Catalyzed Carbene Chemistry. *ACS Catal.* **2018**, *8*, 10676−10682. (b) Berry, J. F.; Lu, C. C. Metal-Metal Bonds: From Fundamentals to Applications. *Inorg. Chem.* **2017**, *56*, 7577−7581. (c) Karunananda, M. K.; Mankad, N. P. Heterobimetallic H_2 addition and alkene/alkane elimination reactions related to the mechanism of E-selective alkyne semihydrogenation. *Organometallics* **2017**, *36*, 220−227. (d) Wu, B.; Wilding, M. J. T.; Kuppuswamy, S.; Bezpalko, M. W.; Foxman, B. M.; Thomas, C. M. Exploring Trends in Metal-Metal Bonding, Spectroscopic Properties, and Conformational Flexibility in a Series of Heterobimetallic Ti/M and V/M Complexes (M = Fe, Co, Ni, and Cu). *Inorg. Chem.* **2016**, *55*, 12137−12148. (e) Beach, S. A.; Doerrer, L. H. Heterobimetallic Lantern Complexes and Their Novel Structural and Magnetic Properties. *Acc. Chem. Res.* **2018**, *51*, 1063−1072. (f) Powers, I. G.; Uyeda, C. Metal-Metal Bonds in Catalysis. *ACS Catal.* **2017**, *7*, 936−958. (g) Huang, G.-H.; Li, J.-M.; Huang, J.-J.; Lin, J.-D.; Chuang, G. J. Cooperative effect of two metals: $CoPd(OAc)_4$-catalyzed C-H amination and aziridination. *Chem. - Eur. J.* **2014**, *20*, 5240−5243. (h) Corcos, A. R.; Pap, J. S.; Yang, T.; Berry, J. F. A Synthetic Oxygen Atom Transfer Photocycle from a Diruthenium Oxyanion Complex. *J. Am. Chem. Soc.* **2016**, *138*, 10032−10040.

(5) (a) Pakula, R. J.; Srebro-Hooper, M.; Fry, C. G.; Reich, H. J.; Autschbach, J.; Berry, J. F. Palladium Acetate Revisited: Unusual Ring-Current Effects, One-Electron Reduction, and Metal-Metal Bonding. *Inorg. Chem.* **2018**, *57*, 8046−8049. (b) Peng, Q.; Yan, H.; Zhang, X.; Wu, Y.-D. Conjugate Addition vs Heck Reaction: A Theoretical Study on Competitive Coupling Catalyzed by Isoelectronic Metal (Pd(II) and Rh(I)). *J. Org. Chem.* **2012**, *77*, 7487−7496.

(6) Umakoshi, K.; Ichimura, A.; Kinoshita, I.; Ooi, S. The dinuclear palladium(II) complex of pyridine-2-thiol. Synthesis, structure, and electrochemistry. *Inorg. Chem.* **1990**, *29* (20), 4005−4010.

(7) (a) Nakanishi, I.; Matsumoto, K.; Ooi, S. Structures of benzenethiolato complexes of palladium(II) and platinum(II). *Acta Crystallogr., Sect. C: Cryst. Struct. Commun.* **1991**, *C47*, 2073−2076. (b) Lingen, V.; Luening, A.; Strauss, C.; Pantenburg, I.; Deacon, G. B.; Klein, A.; Meyer, G. Palladium Complexes with the $SC_6F_4H_4$ Ligand - Synthesis, Spectroscopy, and Structures. *Eur. J. Inorg. Chem.* **2013**, *2013*, 4450−4458. (c) Hua, R.; Takeda, H.; Onozawa, S.; Abe, Y.; Tanaka, M. Palladium-catalyzed thioesterification of alkynes with O-methyl S-phenyl thiocarbonate. *J. Am. Chem. Soc.* **2001**, *123*, 2899−2900.

(8) (a) Halder, P.; Dey, A.; Paine, T. K. Molecular and electronic structure of a nonheme iron(II) model complex containing an iron-carbon bond. *Inorg. Chem.* **2009**, *48* (24), 11501−11503. (b) Mizota, M.; Yokoyama, Y.; Sakai, K. Tetrakis[pyridine-2-(1*H*)-thion-k*S*]-platinum(II) dichloride. *Acta Crystallogr., Sect. E: Struct. Rep. Online* **2005**, *61*, m1433−m1435. (c) Halder, P.; Ghorai, S.; Banerjee, S.; Mondal, B.; Rana, A. Iron(II) complexes of 2-mercaptopyridine as rubredoxin site analogues. *Dalton Trans* **2017**, *46*, 13739−13744. (d) Han, Z.; Shen, L.; Brennessel, W. W.; Holland, P. L.; Eisenberg, R. Nickel Pyridinethiolate Complexes as Catalysts for the Light-Driven Production of Hydrogen from Aqueous Solutions in Noble-Metal-Free Systems. *J. Am. Chem. Soc.* **2013**, *135*, 14659−14669. (e) Halder, P.; Paine, T. K. Synthesis and reactivity of cobalt complexes derived from tris(2-pyridylthio)methane ligand: structural characterization of cobalt-(III) complexes containing cobalt-carbon bond. *Indian J. Chem.* **2011**, *50A*, 1394−1402.

(9) (a) Kitano, K. i.; Tanaka, R.; Kimura, T.; Tsuda, T.; Shimizu, S.; Takagi, H.; Nishioka, T.; Shiomi, D.; Ichimura, A.; Kinoshita, I.; Isobe, K.; Ooi, S. i. Lantern-type dinuclear $Cr^{III}Pt^{II}$ and $V^{IV}Pt^{II}$ complexes bridged by pyridine-2-thiolate. Synthesis and characterization. *Dalton Trans* **2000**, 995−1000. (b) Kitano, K. i.; Tanaka, K.; Nishioka, T.; Ichimura, A.; Kinoshita, I.; Isobe, K.; Ooi, S. i. Lantern type heterobimetallic complexes. Tetra-m-4-methylpyridine-2-thiolato bridged platinum(II) cobalt(II) and oxidation complexes. *J. Chem. Soc., Dalton Trans.* **1998**, 3177−3182.

(10) Wachtler, E.; Oro, L. A.; Iglesias, M.; Gerke, B.; Pottgen, R.; Gericke, R.; Wagler, J. Synthesis and Oxidation of a Paddlewheel-Shaped Rhodium/Antimony Complex Featuring Pyridine-2-Thiolate Ligands. *Chem. - Eur. J.* **2017**, *23*, 3447−3454.

(11) (a) Nippe, M.; Turov, Y.; Berry, J. F. Remote Effects of Axial Ligand Substitution in Heterometallic Cr≡Cr···M Chains. *Inorg. Chem.* **2011**, *50*, 10592−10599. (b) Liu, Y.-C.; Hua, S.-A.; Cheng, M.-C.; Yu, L.-C.; Demeshko, S.; Dechert, S.; Meyer, F.; Lee, G.-H.; Chiang, M.-H.; Peng, S.-M. Electron Delocalization of Mixed-Valence Diiron Sites Mediated by Group 10 Metal Ions in Heterotrimetallic Fe-M-Fe (M = Ni, Pd, and Pt) Chain Complexes. *Chem. - Eur. J.* **2018**, *24*, 11649−11666.

DOI: 10.1021/acs.inorgchem.8b03568
Inorg. Chem. 2019, 58, 2270−2274

(12) Hua, S.-A.; Cheng, M.-C.; Chen, C.-H.; Peng, S.-M. From Homonuclear Metal String Complexes to Heteronuclear Metal String Complexes. *Eur. J. Inorg. Chem.* **2015**, *2015*, 2510−2523.
(13) (a) Gramigna, K. M.; Oria, J. V.; Mandell, C. L.; Tiedemann, M. A.; Dougherty, W. G.; Piro, N. A.; Kassel, W. S.; Chan, B. C.; Diaconescu, P. L.; Nataro, C. Palladium(II) and Platinum(II) Compounds of 1,1′- Bis(phosphino)metallocene (M = Fe, Ru) Ligands with Metal−Metal Interactions. *Organometallics* **2013**, *32*, 5966−5979. (b) Blass, B. L.; Hernandez Sanchez, R.; Decker, V. A.; Robinson, M. J.; Piro, N. A.; Kassel, W. S.; Diaconescu, P. L.; Nataro, C. Structural, Computational, and Spectroscopic Investigation of $[Pd(\kappa^3\text{-}1,1'\text{-bis(di-tert-butylphosphino)ferrocenediyl})X]^+$ (X = Cl, Br, I) Compounds. *Organometallics* **2016**, *35*, 462−470. (c) Klapp, L. R. R.; Bruhn, C.; Leibold, M.; Siemeling, U. Ferrocene-Based Bis(guanidines): Superbases for Tridentate N,Fe,NCoordination. *Organometallics* **2013**, *32*, 5862−5872. (d) Abubekerov, M.; Khan, S. I.; Diaconescu, P. L. Ferrocene-bis(phosphinimine) Nickel(II) and Palladium(II) Alkyl Complexes: Influence of the Fe−M (M = Ni and Pd) Interaction on Redox Activity and Olefin Coordination. *Organometallics* **2017**, *36*, 4394−4402. (e) Jess, K.; Baabe, D.; Bannenberg, T.; Brandhorst, K.; Freytag, M.; Jones, P. G.; Tamm, M. Ni−Fe and Pd−Fe Interactions in Nickel(II) and Palladium(II) Complexes of a Ferrocene-Bridged Bis(imidazolin-2-imine) Ligand. *Inorg. Chem.* **2015**, *54*, 12032−12045. (f) Metallinos, C.; Tremblay, D.; Barrett, F. B.; Taylor, N. J. 1,1'-Bis(phosphoranylidenamino)ferrocene palladium(II) complexes: An unusual case of dative Fe-Pd bonding. *J. Organomet. Chem.* **2006**, *691*, 2044−2047.
(14) Lubben, M.; Meetsma, A.; Wilkinson, E. C.; Feringa, B.; Que, L., Jr. Nonheme iron centers in oxygen activation: characterization of an iron(III) hydroperoxide intermediate. *Angew. Chem., Int. Ed. Engl.* **1995**, *34*, 1512−1514.
(15) Geersing, A.; Segaud, N.; van der Wijst, M. G. P.; Rots, M. G.; Roelfes, G. Importance of Metal-Ion Exchange for the Biological Activity of Coordination Complexes of the Biomimetic Ligand N4Py. *Inorg. Chem.* **2018**, *57*, 7748−7756.
(16) Berry, J. F. Two-Center/Three-Electron Sigma Half-Bonds in Main Group and Transition Metal Chemistry. *Acc. Chem. Res.* **2016**, *49*, 27−34.

DOI: 10.1021/acs.inorgchem.8b03568
Inorg. Chem. 2019, 58, 2270−2274